Inorganica Chimica Acta 381 (2012) 170–180

Contents lists available at SciVerse ScienceDirect

Inorganica Chimica Acta

journal homepage: www.elsevier.com/locate/ica

Bis(2-pyridylmethyl)alkyl(thioalkyl)diamines as promising scaffolds for the construction of fluorescent and redox chemosensors for transition and post-transition metal ions

Riccardo Montis [a], M. Carla Aragoni [a], Massimiliano Arca [a], Carla Bazzicalupi [b], Alexander J. Blake [c], Claudia Caltagirone [a], Greta De Filippo [a], Alessandra Garau [a,*], Paola Gratteri [d], Francesco Isaia [a], Vito Lippolis [a,*], Anna Pintus [a]

[a] *Dipartimento di Chimica Inorganica ed Analitica, Università degli Studi di Cagliari, S.S. 554 Bivio per Sestu, I-09042 Monserrato (CA), Italy*
[b] *Dipartimento di Chimica "Ugo Schiff", Università degli Studi di Firenze, Polo Scientifico, Via della Lastruccia 3, I-50019 Sesto Fiorentino (FI), Italy*
[c] *School of Chemistry, The University of Nottingham, University Park, Nottingham NG7 2RD, UK*
[d] *Laboratory of Molecular Modeling Cheminformatics & QSAR, Dipartimento di Scienze Farmaceutiche, Università degli Studi di Firenze, Polo Scientifico, Via U. Schiff, I-50019 Sesto Fiorentino (FI), Italy*

ARTICLE INFO

Article history:
Available online 22 September 2011

Fluorescence Spectroscopy: from Single Chemosensors to Nanoparticles Science – Special Issue

Keywords:
Aminopyridine ligands
Fluorescent chemosensors
Zinc
Cadmium
Quinoline
Dansyl

ABSTRACT

N,N′-Bis(2-pyridylmethyl)propylendiamine (**1**) and *N,N′-bis*(2-pyridylmethyl)-1,5-diamino-3-thiapentane (**2**) have been functionalised at the secondary nitrogen atoms with dansylamidoethyl ($\mathbf{L^1}$, $\mathbf{L^3}$), 2-quinolinylmethyl ($\mathbf{L^2}$, $\mathbf{L^4}$) and ferrocenylmethyl ($\mathbf{L^6}$, $\mathbf{L^7}$) pendant arms with the intention to study their potentiality as receptor units in molecular sensors. The optical response of $\mathbf{L^1}$–$\mathbf{L^4}$ to the presence of the metal ions Cu^{2+}, Zn^{2+}, Cd^{2+}, Hg^{2+} and Pb^{2+} has been investigated in MeCN/H_2O (4:1 v/v) solution. The electrochemical response of $\mathbf{L^6}$ and $\mathbf{L^7}$ to the presence of the same metal ions has been investigated in anhydrous MeCN/CH_2Cl_2 10:1 (v/v) solution. Results are compared and discussed with the aim to clarify the mutual role played by the *bis*(2-methylpyridyl)alkyl(thioalkyl)diamines and the signalling units attached to them in reaching the selectivity of the responses observed.

1. Introduction

The development of selective and sensitive analytical tools for rapid monitoring of transition and post-transition metal ions is of particular interest, since many of these metals are either pollutants in environmental systems or essential trace elements in biological systems. In particular, luminescence quenching or enhancement following the interaction between chemically engineered fluorescent molecules and the targeted metal ions is revealing an effective and simple solution to complex analytical problems [1–21].

From a structural point of view, according to the simple "receptor–spacer–fluorophore" supramolecular modular scheme, the most common class of fluorescent chemosensors (conjugated chemosensors) consists of a fluorogenic unit (signalling site) covalently linked, through an appropriate spacer, to a guest-binding site (receptor unit). The selective host–guest interaction of the target species with the receptor unit (recognition event) is converted into an enhancement or quenching of the fluorophore emission brought about by the perturbation of such photoinduced processes as energy transfer, charge transfer, electron transfer, or the formation or disappearance of excimers and exciplexes. However, the choice of the "read-out" or signalling unit can be critical to both the performance and the selectivity of the sensor, especially if a direct interaction of the fluorophore with the target species is possible (for example, the signalling unit possesses appropriate coordinating donor atoms for the metal ion species).

Important aspects of the design of fluorescent chemosensors for metal ions therefore include analyte affinity, choice of chromophore or fluorophore, binding selectivity and transduction signalling mechanism. All these aspects can in principle be targeted by changing the receptor, the signalling and the spacer units, taking advantage of the extensive knowledge available from classical coordination chemistry, as well as by choosing the medium (the solvent or the pH of the solution, for instance) in which the host–guest interaction takes place [1–21].

* Corresponding authors. Tel.: +39 070 675 4450; fax: +39 070 675 4456 (A. Garau), tel.: +39 070 675 4467; fax: +39 070 675 4456 (V. Lippolis).
E-mail addresses: agarau@unica.it (A. Garau), lippolis@unica.it (V. Lippolis).

0020-1693 © 2011 Elsevier B.V. Open access under CC BY license.
doi:10.1016/j.ica.2011.09.025

Similar considerations apply to any other type of chemosensor for metal ions based on the synthetic modular scheme outlined above, but making use of signalling units not necessarily involving an optic transduction mechanism of the host–guest interaction.

In this context, we have considered *N*,*N*′-*bis*(2-pyridylmethyl)propylendiamine (**1**) and *N*,*N*′-*bis*(2-pyridylmethyl)-1,5-diamino-3-thiapentane (**2**) as metal ion binding platforms for the construction of the fluorescent chemosensors $\mathbf{L^1}$–$\mathbf{L^4}$ (Scheme 1) *via* functionalization of the secondary amine groups with coordinating dansylamidoethyl ($\mathbf{L^1}$, $\mathbf{L^3}$) or 2-quinolinylmethyl ($\mathbf{L^2}$, $\mathbf{L^4}$) pendant arms. The compound $\mathbf{L^5}$ featuring the 1,7-diaza-4-thiacyclononane ([9]aneN_2S, **3**) was also synthesized for comparison purposes. Both tetradentate **1** and pentadentate **2** belong to the well known class of aminopyridine ligands whose coordination chemistry has been widely studied [22–27], but the use as receptor units in fluorescent chemosensors is limited to only few members of the family such as *bis*(2-picolyl)amine [28]. They present relatively soft donor centres at the pyridine rings (borderline base) with predisposition, therefore, to combine with late transition and post-transition heavy metals. In this respect, the optical response of $\mathbf{L^1}$–$\mathbf{L^5}$ to the presence of Cu^{2+}, Zn^{2+}, Cd^{2+}, Hg^{2+} and Pb^{2+} has been investigated in MeCN/H_2O (4:1 v/v) solution. Furthermore, the potential use of **1** and **2** as binding units in redox chemosensors has also been considered by the synthesis of $\mathbf{L^6}$ and $\mathbf{L^7}$ featuring ferrocenylmethyl pendant arms at the secondary amino groups. The electrochemical response of $\mathbf{L^6}$ and $\mathbf{L^7}$ to the presence of the above-mentioned metal ions has been investigated in anhydrous MeCN/CH_2Cl_2 10:1 (v/v) solution, and compared to the optical response of $\mathbf{L^1}$–$\mathbf{L^4}$ in order to possibly analyze the role played by the receptor units represented by **1** and **2** in the responses observed for the two types of chemosensors, to the presence of the considered metal ions.

2. Experimental

All melting points are uncorrected. Microanalytical data were obtained using a Fison EA CHNS-O instrument operating at

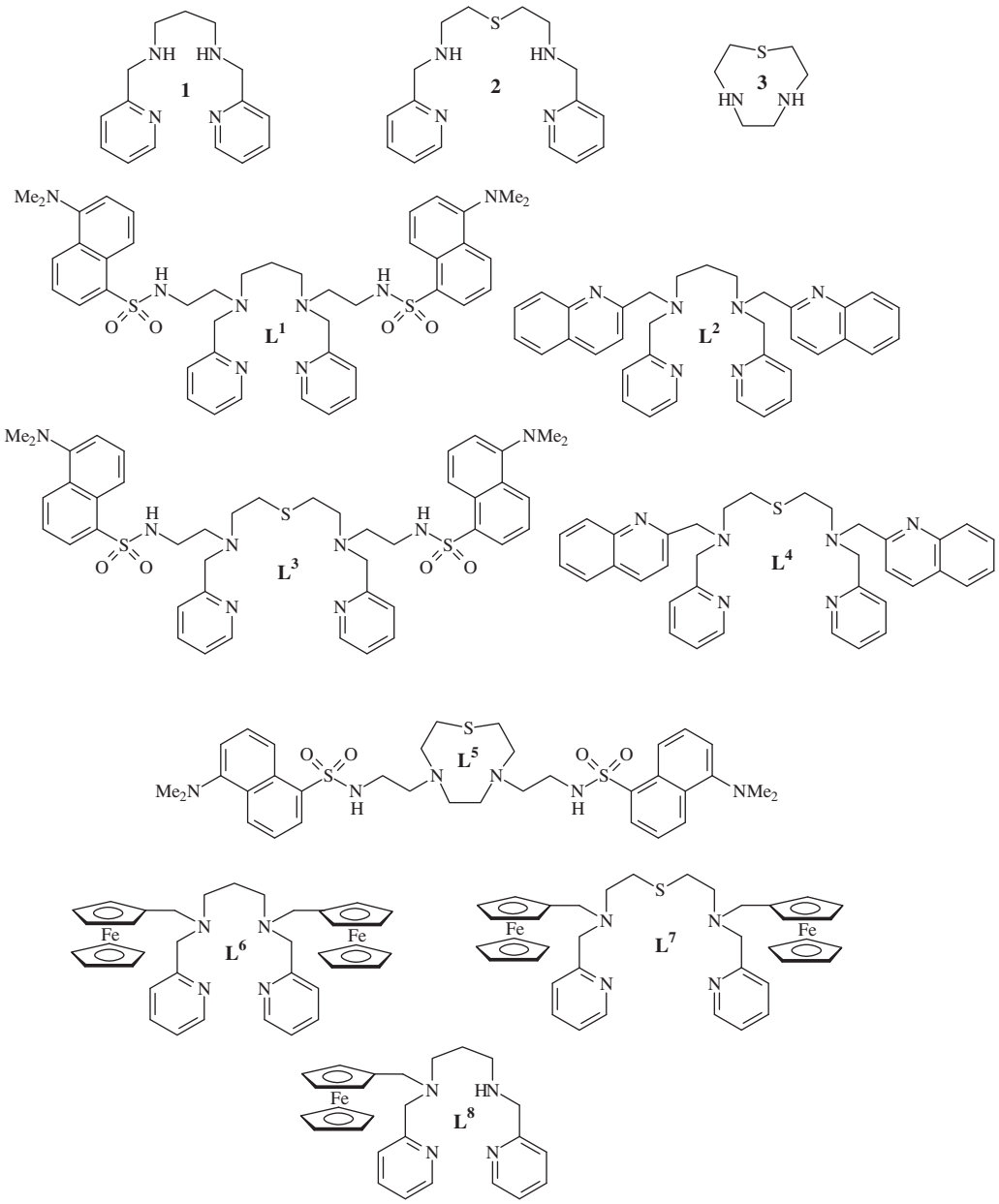

Scheme 1. Ligands considered in this paper.

1000 °C. ESI mass spectra were recorded on a Hewlett Packard mass-spectrometer model 5989 A. ^{1}H and ^{13}C NMR spectra were recorded on a Varian VXR300 or a Varian VXR400 spectrometer. The spectrophotometric measurements were carried out at 25 °C using a Varian model Cary 5 UV–Vis–NIR spectrophotometer and a Thermo Nicolet Evolution 300 spectrophotometer. Uncorrected emission, and corrected excitation spectra were obtained with a Varian Cary Eclipse Fluorescence spectrophotometer. In order to allow comparison among emission intensities, we performed corrections for instrumental response, inner filter effect, and phototube sensitivity [29]. A correction for differences in the refraction index was introduced when necessary [29]. Luminescence quantum yields (uncertainty ± 15%) were determined using quinine sulphate in 0.5 M H_2SO_4 aqueous solution (Φ = 0.546) as a reference. For spectrophotometric measurements MeCN (Uvasol, Merck) and Millipore grade water were used as solvents. Spectrofluorimetric titrations of **L^1**–**L^5** with metal ions were performed by adding increasing volumes of a solution of the metal ion in MeCN to a solution of the ligand (3 mL) in MeCN/H_2O (4:1 v/v, 25 °C), buffered at pH 7.0 with 1 M MOPS [3-(*N*-morpholino)propanesulfonic acid] (3 μL, H_2O solution). Solutions of the ligands in MeCN/H_2O (4:1 v/v) were 3.0–3.5 × 10^{-5} M, and those of the metals in MeCN were 2.5 × 10^{-3} M. In all cases the effect of dilution on fluorescence emission was neglected.

Solvents and starting materials were purchased from commercial sources where available. The compounds *N,N′-bis*(2-pyridylmethyl)propylendiamine (**1**) [30], *N,N′-bis*(2-pyridylmethyl)-1,5-diamino-3-thiapentane (**2**) [31], 1,7-diaza-4-thiacyclononane (**3**) [32], (ferrocenylmethyl)trimethylammonium iodide [33] and dansylamidoethyl chloride [34] were synthesized according to the reported procedures.

2.1. Synthesis of N,N′-bis(dansylamidoethyl)-N,N′-bis(2-pyridylmethyl)propylendiamine (L^1)

A solution of dansylamidoethyl chloride (1.22 g, 3.90 mmol) in dry MeCN (15 mL) was added dropwise to a mixture of *N,N′-bis*(2-pyridylmethyl)propylendiamine (**1**) (0.50 g, 1.95 mmol) and K_2CO_3 (1.35 g, 9.75 mmol) in dry MeCN (50 mL). The mixture was maintained at room temperature for 24 h under nitrogen. The solid was filtered off, the solvent was removed under reduced pressure and the oily residue was washed with diethylether to obtain a yellow solid (1.26 g, yield 80%). Mp: 50 °C. Elem. *Anal.* Calc. for $C_{43}H_{52}N_8O_4S_2$): C, 63.8; H, 6.5; N, 13.8; S, 7.9. Found: C, 63.5; H, 6.3; N, 13.5; S, 7.7. ^{1}H NMR (300 MHz, $CDCl_3$): δ_H 2.16 (t, 2H, *J* = 7.2 Hz, NCH_2CH_2), 2.44 (t, 4H, *J* = 7.2 Hz, NCH_2CH_2), 2.83 (m, 20H, NCH_2CH_2Ndans, NCH_2CH_2Ndans and NCH_3), 3.47 (s, 4H, NCH_2Py), 7.11 (m, 8H), 7.46 (m, 4H), 8.18 (d, 2H, *J* = 7.6 Hz,), 8.34 (d, 2H, *J* = 7.6 Hz), 8.46 (d, 2H, *J* = 8.4 Hz), 8.52 (m, 2H). ^{13}C NMR (100 MHz, $CDCl_3$): δ_c 24.26 (NCH_2CH_2), 40.77 (NCH_2CH_2Ndans), 45.01 (NCH_3), 51.91 (NCH_2CH_2), 52.80 (NCH_2CH_2Ndans), 58.88 (NCH_2Py), 114.61, 118.91, 121.74, 122.44, 122.77, 127.56, 128.91, 129.37, 129.43, 129.59, 134.81, 136.19, 148.67, 151.36, 158.72 (aromatic carbons). UV–Vis spectrum (MeCN/H_2O 4:1 v/v, 25 °C): λ (ε) 254 (33 790), 338 nm (9960 dm^3 mol^{-1} cm^{-1}). Mass spectrum EI$^+$: *m*/*z* 808 ([$C_{43}H_{52}N_8O_4S_2$]$^+$).

2.2. Synthesis of N,N′-bis(2-quinolinylmethyl)-N,N′-bis(2-pyridylmethyl)propylendiamine (L^2)

2-(Chloromethyl)quinoline (0.84 g, 3.91 mmol) was added to a mixture of **1** (0.50 g, 1.96 mmol) and K_2CO_3 (1.62 g, 7.81 mmol) in dry MeCN (90 mL). The mixture was heated to reflux for 24 h under nitrogen. The solid was filtered off and the solvent was removed under reduced pressure. The residue was crystallized from *n*-hexane to obtain a light brown solid (0.92 g, yield 87%). Mp: 122 °C. Elem. *Anal.* Calc. for $C_{35}H_{34}N_6$: C, 78.0; H, 6.4; N, 15.6. Found: C, 77.7; H, 6.5; N, 15.5%. ^{1}H NMR (400 MHz, $CDCl_3$): δ_H 1.79 (t, 2H, *J* = 6.8 Hz, NCH_2CH_2), 2.53 (t, 4H, *J* = 6.8 Hz, NCH_2CH_2), 3.71 (s, 4H, NCH_2Py), 3.82 (s, 4H, NCH_2q), 7.43 (m, 7H), 7.59–7.66 (m, 7H), 7.84 (d, 2H, *J* = 8.0 Hz), 7.94 (d, 2H, *J* = 8.0 Hz), 8.39 (d, 2H, *J* = 8.0 Hz). ^{13}C NMR (75 MHz, $CDCl_3$): δ_c 24.7 (NCH_2CH_2), 52.4 (NCH_2CH_2), 60.5 (NCH_2Py), 61.1 (NCH_2q), 120.7, 121.7, 122.7, 125.9, 127.2, 127.4, 128.9, 129.2, 136.1, 136.2, 147.4, 148.8, 159.7, 160.6. UV–Vis spectrum (MeCN/H_2O 4:1 v/v, 25 °C): λ (ε) 230 (68 600), 262 (13 650), 303 (7000), 315 nm (8400 dm^3 mol^{-1} cm^{-1}). Mass spectrum EI$^+$: *m*/*z* 538 ([$C_{35}H_{34}N_6$]$^+$).

2.3. Synthesis of N,N′-bis(dansylamidoethyl)-N,N′-bis(2-pyridylmethyl)-1,5-diamino-3-thiapentane (L^3)

A solution of dansylamidoethyl chloride (0.98 g, 3.12 mmol) in dry MeCN (100 mL) was added dropwise to a mixture of *N,N′-bis*(2-pyridylmethyl)-1,5-diamino-3-thiapentane (**2**) (0.47 g, 1.56 mmol) and K_2CO_3 (1.07 g, 7.81 mmol) in dry MeCN (50 mL). The mixture was maintained at room temperature for 24 h under nitrogen. The solid was filtered off, the solvent was removed under reduced pressure and the oily residue was washed with diethylether to obtain a yellow solid (0.95 g, yield 71%). Mp: 55 °C. Elem. *Anal.* Calc. for $C_{44}H_{54}N_8O_4S_3$: C, 61.8; H, 6.4; N, 13.1; S, 11.3. Found: C, 60.5; H, 6.6; N, 12.8; S, 12.9%. ^{1}H NMR (300 MHz, $CDCl_3$): δ_H 2.25 (t, 4H, *J* = 7.2 Hz, NCH_2CH_2S), 2.45 (t, 4H, *J* = 7.2 Hz, NCH_2CH_2S), 2.57 (t, 4H, *J* = 7.2 Hz, NCH_2CH_2Ndans), 2.83 (m, 16H, NCH_2CH_2Ndans and NCH_3), 3.57 (s, 4H, NCH_2Py), 6.82 (s, 2H, NH), 7.10 (m, 8H), 7.45 (m, 4H), 8.18 (d, 2H, *J* = 7.6 Hz,), 8.38 (d, 2H, *J* = 7.6 Hz), 8.51 (d, 2H, *J* = 7.6 Hz). ^{13}C NMR (75 MHz, $CDCl_3$): δ_c 29.86 (NCH_2CH_2), 41.13 (NCH_2CH_2Ndans), 45.27 (NCH_3), 52.65 (NCH_2CH_2), 53.30 (NCH_2CH_2Ndans), 59.27 (NCH_2Py), 114.94, 119.18, 122.10, 122.84, 123.02, 127.89, 129.22, 129.56, 129.69, 129.93, 134.88, 136.49, 148.79, 151.65, 158.49 (aromatic carbons). UV–Vis spectrum (MeCN/H_2O 4:1 v/v, 25 °C): λ (ε) 254 (40 740), 338 nm (10 430 dm^3 mol^{-1} cm^{-1}). Mass spectrum EI$^+$: *m*/*z* 855 ([$C_{44}H_{54}N_8O_4S_3$]$^+$).

2.4. Synthesis of N,N′-bis(2-quinolinylmethyl)-N,N′-bis(2-pyridylmethyl)-1,5-diamino-3-thiapentane (L^4)

2-(Chloromethyl)quinoline (0.71 g, 3.32 mmol) was added to a mixture of **2** (0.50 g, 1.66 mmol) and K_2CO_3 (0.92 g, 6.71 mmol) in dry MeCN (50 mL). The mixture was heated to reflux for 24 h under nitrogen. The solid was filtered off, the solvent was removed under reduced pressure to obtain an orange oil (0.32 g, yield 34%). *Anal.* Calc. for $C_{36}H_{36}N_6S$: C, 73.9; H, 6.2; N, 14.4; S, 5.5. Found: C, 73.8; H, 6.3; N, 14.5; S, 5.3%. ^{1}H NMR (400 MHz, $CDCl_3$): δ_H 1.77 (t, 4H, *J* = 6.8 Hz, NCH_2CH_2S), 2.55 (t, 4H, *J* = 6.8 Hz, NCH_2CH_2S), 3.73 (s, 4H, NCH_2Py), 3.83 (s, 4H, NCH_2q), 7.45 (m, 7H), 7.63 (m, 7H), 7.88 (d, 2H, *J* = 8.0 Hz), 7.96 (d, 2H, *J* = 8.0 Hz), 8.41 (d, 2H, *J* = 8.0 Hz). ^{13}C NMR (100 MHz, $CDCl_3$): δ_c 29.48 (NCH_2CH_2), 53.53 (NCH_2CH_2), 59.87 (NCH_2Py), 60.51 (NCH_2q), 120.67, 121.67, 122.72, 125.76, 126.96, 127.14, 128.49, 129.00, 135.99, 136.05, 147.03, 148.51, 158.91, 159.85. UV–Vis spectrum (MeCN/H_2O 4:1 v/v, 25 °C): λ (ε) 231 (66 060), 263 (11 920), 303 (7320), 315 nm (7690 dm^3 mol^{-1} cm^{-1}). Mass spectrum EI$^+$: *m*/*z* 584 ([$C_{44}H_{54}N_8O_4S_3$]$^+$).

2.5. Synthesis of 4,7-bis(dansylamidoethyl)-1-thia-4,7-diazacyclononane (L^5)

A solution of dansylamidoethyl chloride (0.55 g, 1.76 mmol) in dry MeCN (150 mL) was added dropwise to a mixture of 1,7-diaza-4-thiacyclononane (**3**) (0.13 g, 0.88 mmol) and K_2CO_3 (0.60 g,

4.4 mmol) in dry MeCN (40 mL). The mixture was maintained at room temperature for 48 h under nitrogen. The solid was filtered off, the solvent was removed under reduced pressure and the residue was dissolved in CH_2Cl_2 and washed with water. The organic extracts were dried over Na_2SO_4, filtered and the solvent removed *in vacuo* to give a yellow oil which was purified by flash-chromatography on silica gel using a CH_2Cl_2/MeOH (9:1 v/v) mixture as eluant. A yellow solid was obtained (0.363 g, 59% yield). Mp: 110–112 °C. Elem. *Anal.* Calc. for $C_{34}H_{46}N_6O_4S_3$: C, 58.4; H, 6.6; N, 12.0; S, 13.8. Found: C, 58.5; H, 6.7; N, 12.1; S, 14.0%. ^{1}H NMR (400 MHz, $CDCl_3$): δ_H 2.38 (m, 4H, NCH_2CH_2S), 2.55 (m, 4H, NCH_2CH_2S), 2.67 (s, 4H, NCH_2CH_2N) 2.87 (m, 20H, NCH_2CH_2Ndans, NCH_2CH_2Ndans and NCH_3), 7.16 (d, 2H, J = 7.6 Hz), 7.49 (m, 4H), 8.22 (d, 2H, J = 8.4 Hz), 8.35 (d, 2H, J = 8.4 Hz), 8.52 (d, 2H, J = 8.4 Hz). ^{13}C NMR (100 MHz, $CDCl_3$): δ_c 33.46 (NCH_2CH_2S), 41.33 (NCH_2CH_2Ndans), 45.49 (NCH_3), 55.42 (NCH_2CH_2S), 56.34 (NCH_2CH_2Ndans), 56.83 (NCH_2CH_2N), 115.3, 119.20, 123.24, 128.44, 129.44, 129.77, 129.93, 130.35, 134.92, 151.83 (aromatic carbons). UV–Vis spectrum (MeCN/H_2O 4:1 v/v, 25 °C): λ (ε) 253 (25 850), 340 nm (8300 dm^3 mol^{-1} cm^{-1}). Mass spectrum EI$^+$: m/z 698 ($[C_{34}H_{46}N_6O_4S_3]^+$).

2.6. Synthesis of N,N′-bis(ferrocenylmethyl)-N,N′-bis(2-pyridylmethyl)-propylenediamine (**L^6**)

A solution of (ferrocenylmethyl)trimethylammonium iodide (4.72 g, 12.28 mmol) in anhydrous MeCN (100 mL) was added dropwise to a refluxing solution of **1** (1.17 g, 4.56 mmol) and K_2CO_3 (4.44 g, 32.12 mmol) in anhydrous MeCN (40 mL). The resulting mixture was stirred overnight at 80 °C. K_2CO_3 was then filtered off and washed with hot MeCN (20 mL). The solvent was removed under reduced pressure and the residue was dissolved in CH_2Cl_2 and washed with water. The organic extracts were dried over Na_2SO_4, filtered and the solvent removed *in vacuo*. The residue was washed with Et_2O to afford an orange solid (1.36 g, 45.6% yield). Mp: 110 °C. Elem. *Anal.* Calc. for $C_{37}H_{40}Fe_2N_4$: C, 68.1; H, 6.2; N, 8.6. Found: C, 67.8; H, 6.3; N, 8.4%. ^{1}H NMR (400 MHz, $CDCl_3$): δ 1.60 (t, J = 6.8 Hz, 2H, NCH_2CH_2), 2.33 (t, J = 6.8 Hz, 4H, NCH_2CH_2), 3.42 (s, 4H, NCH_2Fc), 3.58 (s, 4H, NCH_2Py), 4.02 (m, 18H), 7.07 (t, 2H, J = 7.6 Hz), 7.32 (d, 2H, J = 7.6 Hz), 7.55 (t, 2H, J = 7.6 Hz), 8.45 (d, 2H, J = 7.6 Hz). ^{13}C NMR (75 MHz, $CDCl_3$): δ 25.1 (NCH_2CH_2), 51.4 (NCH_2CH_2), 53.3 (NCH_2Fc), 59.6 (NCH_2Py), 67.7, 68.3, 70.0, 82.9 (C ferrocene), 121.6, 122.7, 136.1, 148.7, 161.0 (aromatic carbons). Mass spectrum EI$^+$: m/z 652 ($[C_{37}H_{40}Fe_2N_4]^+$).

2.7. Synthesis of N,N′-bis(ferrocenylmethyl)-N,N′-bis(2-pyridylmethyl)-1,5-diamino-3-thiapentane (**L^7**)

A solution of (ferrocenylmethyl)trimethylammonium iodide (1.51 g, 3.90 mmol) in anhydrous MeCN (100 mL) was added dropwise to a refluxing solution of **2** (0.50 g, 1.66 mmol) and K_2CO_3 (1.83 g, 13.28 mmol) in anhydrous MeCN (40 mL). The resulting mixture was stirred overnight at 80 °C. K_2CO_3 was then filtered off and washed with hot MeCN (20 mL). The solvent was removed under reduced pressure and the residue was dissolved in CH_2Cl_2 and washed with water. The organic extracts were dried over Na_2SO_4, filtered and the solvent removed *in vacuo* to yield a brown oil (0.37 g, 32.0% yield). Elem. *Anal.* Calc. for $C_{38}H_{42}Fe_2N_4S$: C, 65.3; H, 6.1; N, 8.0; S, 4.6. Found: C, 65.1; H, 6.2; N, 7.9; S, 4.4%. ^{1}H NMR (400 MHz, $CDCl_3$): δ 2.70 (t, J = 6.8 Hz, 2H, NCH_2CH_2S), 2.85 (t, J = 6.8 Hz, 4H, NCH_2CH_2), 3.43 (s, 4H, NCH_2Fc), 3.59 (s, 4H, NCH_2Py), 4.10 (m, 18H), 7.08 (t, 2H, J = 7.6 Hz), 7.35 (d, 2H, J = 7.6 Hz), 7.58 (t, 2H, J = 7.6 Hz), 8.65 (d, 2H, J = 7.6 Hz). ^{13}C NMR (75 MHz, $CDCl_3$): δ 29.7 (NCH_2CH_2S), 52.9 (NCH_2CH_2), 53.1 (NCH_2Fc), 59.1 (NCH_2Py), 67.7, 68.1, 69.7, 82.3 (C ferrocene), 121.5, 122.5, 135.9, 148.5, 159.5 (aromatic carbons). Mass spectrum EI$^+$: m/z 698 ($[C_{38}H_{42}Fe_2N_4S]^+$).

2.8. Synthesis of [Cu**L^8**$(ClO_4)_2$]

A solution of $Cu(ClO_4)_2{\cdot}2H_2O$ (0.0055 g, 0.0158 mmol) in MeCN (2 mL) was added to a solution of **L^6** (0.0103 g, 0.0158 mmol) in MeCN (10 mL). The resulting mixture was stirred at room temperature for 2 h. The solvent was partially removed under reduced pressure. Dark purple crystals of [Cu**L^8**$(ClO_4)_2$] (see below Section 3.2) were obtained by slow diffusion of Et_2O vapour into the resulting mixture (0.006 g, 53% yield). Elem. *Anal.* Calc. for $C_{26}H_{30}Cl_2CuFeN_4O_8$: C, 43.6; H, 4.2; N, 7.8. Found: C, 43.8; H, 4.1; N, 7.8%. UV–Vis spectrum (MeCN, 25 °C): λ (ε) 260 (9560), 293sh (4000), 570sh (210), 625 nm (230 dm^3 mol^{-1} cm^{-1}).

2.9. Cyclic voltammetry

Cyclic voltammetry experiments were recorded at a scan rate of 100 mV s^{-1}, using a conventional three-electrode cell, consisting of a combined working and counter platinum electrode and a standard Ag/AgCl (in KCl 3.5 mol dm^{-3}; 0.2223 V at 25 °C) reference electrode. The experiments were performed at 25 °C in anhydrous MeCN/CH_2Cl_2 10:1 (v/v) mixture. The solutions were about 1.0×10^{-3} mol dm^{-3} in the electroactive species (**L^6** or **L^7**) with n-Bu_4NBF_4 (0.1 mol dm^{-3}) as supporting electrolyte. A stream of argon was passed through the solution prior to the scan. For each redox-responsive ionophore (**L^6** or **L^7**), different solutions were prepared containing increasing amounts of the metal guest cation as hydrated perchlorate or tetrafluoroborate salt (molar ratio ranging from 0 to 1:1) and the cyclic voltammogram was recorded for each solution. Data were recorded on a computer-controlled Autolab PG STAT 100 potentiostat–galvanostat using model GPES electrochemical analysis software.

2.10. Crystallography

Crystal data for [Cu**L^8**$(ClO_4)_2$]: $C_{26}H_{30}Cl_2CuFeN_4O_8$, M = 716.83, triclinic, a = 8.6927(13), b = 10.942(2), c = 15.568(2) Å, α = 72.554(2), β = 79.261(2), γ = 80.205(2)°, U = 1377.6(4) Å^3, T = 150(2) K, space group $P\bar{1}$ (No. 2), Z = 2, μ(Mo Kα) = 1.551, D_{calc} = 1.728 g cm^{-3}. 12 118 reflections [6077 unique with R_{int} = 0.040, 4498 with $I > 2\sigma(I)$] were collected on a Bruker SMART1000 CCD area detector diffractometer using ω-scans. Intensities were corrected for Lorentz-polarization effects and for absorption using multi-scan corrections (T_{min} 0.470, T_{max} 0.661) [35]. The structure was solved by direct methods using *SIR*92 [36], followed by difference Fourier synthesis and refined by full-matrix least-squares on F^2 using SHELXL [35]. All non-H atoms were refined anisotropically and H atoms were introduced at calculated positions and thereafter incorporated into a riding model with $U_{iso}(H)$ = 1.2 U_{eq}(C). At final convergence R_1 [$I > 2\sigma(I)$] = 0.0362 and wR_2 [all data] = 0.0890 for 379 refined parameters; S = 0.95.

2.11. DFT calculations

Quantum-chemical calculations based on Density Functional Theory (DFT) [37] were performed on the 1:1 Zn^{2+} complex of **L^2** in the gas phase with the ligand adopting three possible conformations in the coordination to the metal centre. The GAUSSIAN09 (Rev. A.02) suite of programs was used [38], adopting the mPW1PW [39] hybrid functional. Schäfer, Horn and Ahlrichs double-ζ plus polarisation all-electron basis sets [40] were used for C, H, and N, whereas the LanL08 BS's with relativistic effective core potentials (RECP) were adopted for the heavier Zn, providing in addition d-type polarization functions [41]. The geometry optimizations were

performed without introducing any structural simplification or symmetry restraint, and by adopting a tight SCF convergence criterion (*SCF = tight* keyword). All calculations were carried out on a 64 bit E4 workstation equipped with four quadcore AMD Opteron processors and 16 Gb of RAM, and running the OpenSuSE 10.3 Linux operating system.

A molecular modelling investigation of the 1:1 Zn^{2+} complex of **L²** with an implicit simulation of the MeCN environment was also carried out. In this case a conformational search by means of a molecular dynamics procedure (T = 800 K, 200 saved conformations) was first carried out on each complex by means of an empirical force field method (OPLS2005) [42]. The lowest-energy conformers so obtained were then minimized at the DFT/B3LYP [43] level of theory using the LAV3P** basis set, which uses an effective core potential for metal atoms, as implemented in the software JAGUAR [44], and an implicit simulation of the MeCN environment by the Poisson–Boltzmann equation [45].

3. Results and discussion

3.1. Optical response of L¹, L³ and L⁵ to the presence of Cu^{2+}, Zn^{2+}, Cd^{2+}, Hg^{2+} or Pb^{2+}

The optical response of **L¹**, **L³** and **L⁵** to the presence of Cu^{2+}, Zn^{2+}, Cd^{2+}, Hg^{2+} or Pb^{2+} was studied in MeCN/H_2O (4:1 v/v, 25 °C) solutions buffered with MOPS [MOPS = 3-(*N*-morpholino)propanesulfonic acid] at pH 7.0. The absorption spectra of all three dansylamidopropyl derivatives exhibit a large and unstructured band at around 338 nm and a more intense one at 254 nm (see Section 2). These species are also luminescent, exhibiting emission bands at 528 (**L¹** and **L³**, λ_{exc} = 338 nm) and 540 nm (**L⁵**, λ_{exc} = 340 nm) with a fluorescent quantum yield, Φ, of 0.17 and 0.18 and 0.15 for **L¹**, **L³** and **L⁵**, respectively. Significant and similar changes in the UV–Vis spectra of **L¹**, **L³** and **L⁵** were only observed upon addition of Cu^{2+}, Hg^{2+} or Pb^{2+} to a MeCN/H_2O (4:1 v/v, 25 °C) solution of each ligand buffered at pH 7.0 (see Supplementary material, Figs. S1–S3). In particular, the band at around 338 nm shifts to lower wavelengths (330–332 nm) and increases slightly in intensity, while for the band at 254 nm only a slight increase is observed (see Fig. 1a for the spectrophotometric titration of **L¹** with Cu^{2+}). No significant changes were observed in the UV–Vis spectra of the three ligands upon addition of Zn^{2+} or Cd^{2+}. For all three dansylamidopropyl derivatives, a quenching of the luminescence intensity was observed only upon addition of Cu^{2+} [I_{rel} = 12%, 4%, and 17% for **L¹**, **L³** and **L⁵**, respectively] or Hg^{2+} [I_{rel} = 40%, 34%, and 27% for **L¹**, **L³** and **L⁵**, respectively, I_{rel} (%) represents the percentage of the residual fluorescence intensity in correspondence of a M^{2+}/**L** molar ratio of 2], with the formation of 1:1 metal-to-ligand complexes as suggested by the inflection point in the fluorescence intensity/molar ratio plots (see Figs. 1b and 2 for the case of **L¹**, and Supplementary material, Fig. S4, for the cases of **L³** and **L⁵**). In no case was a shift of the emission band observed upon addition of the metal ions.

The strong quenching effect observed with Cu^{2+} can be ascribed to either a dansyl-to-metal energy-transfer (ET) or to a metal-to-dansyl electron-transfer (eT) mechanism [47]. In the case of Hg^{2+}, a contribution to fluorescence quenching from the heavy-atom effect cannot be excluded, while the ET mechanism cannot be effective for this d^{10} ion [47].

It is worth noting that most of the ligands reported in the literature containing the dansyl fluorophore manifest an ON–OFF type fluorescence response to Hg^{2+}, Cu^{2+} or both, as in the case of **L¹**, **L³** and **L⁵**, with the complexation process being concomitant with the deprotonation of the sulfonamide group [47–51]. In some cases an enhancement of the fluorescence intensity in the presence of Zn^{2+} is also observed [50,51]. These data, therefore, indicate that the dansyl group is an appropriate signalling unit to choose when approaching the design of selective fluorescent chemosensor for Hg^{2+} or Cu^{2+}. The selectivity in the optical response is, therefore, heavily determined by the cooperation of the receptor unit in the binding process. In our case, the lack of influence exerted by the sulfur donors in **L³** and **L⁵** on the selectivity of the proposed chemosensors is particularly surprising. In principle, the presence of soft donor atoms in the binding unit should favour interaction with Hg^{2+} and consequently a preferential optical response toward this metal cation. Presumably the sulfur donor in both **L³** and **L⁵** is not much involved in metal coordination. The metal ions essentially experience an N_4 coordination mode from the aminopyridine frameworks of **L³** similar to that imposed by **L¹**. Furthermore, on comparing the optical responses of **L¹**, **L³** and **L⁵** towards Cu^{2+} and Hg^{2+}, it appears that the metal coordination of the pyridine units in the case of **L¹** and **L³** significantly increases the quenching effect of Cu^{2+} with respect to Hg^{2+}.

3.2. Optical response of L² and L⁴ to the presence of Cu^{2+}, Zn^{2+}, Cd^{2+}, Hg^{2+} or Pb^{2+}

The absorption spectra of MeCN/H_2O (4:1 v/v) solutions of **L²** and **L⁴** exhibit a large unstructured band at around 230 nm and

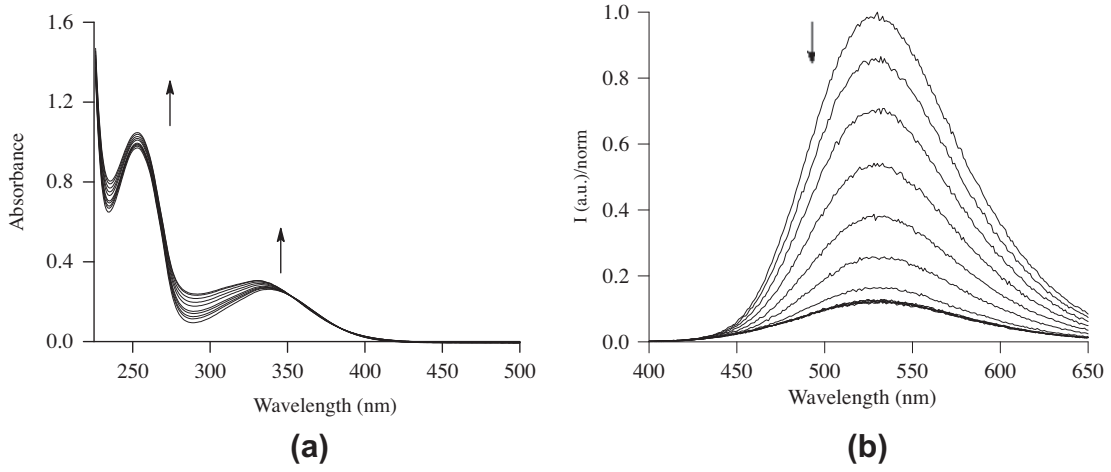

Fig. 1. (a) Changes in the absorption spectrum of **L¹** (3.5×10^{-5} M, MeCN/H_2O 4:1 v/v, pH 7.0, 25 °C) upon addition of increasing amounts of Cu^{2+} and (b) changes in the emission spectrum of **L¹** (3.5×10^{-5} M, MeCN/H_2O 4:1 v/v, pH 7.0, 25 °C, λ_{ex} = 338, λ_{em} = 528 nm) upon addition of increasing amounts of Cu^{2+}.

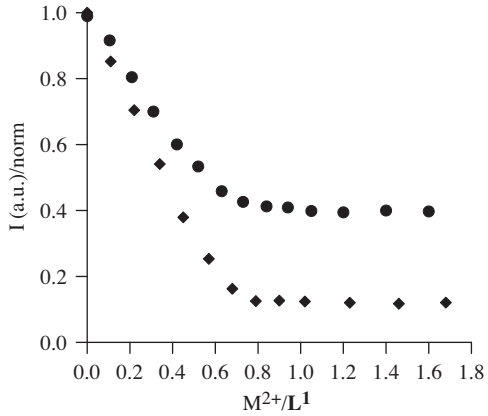

Fig. 2. Normalized fluorescent intensity/molar ratio plots for $\mathbf{L^1}$ (3.5×10^{-5} M, MeCN/H_2O 4:1 v/v, pH 7.0, 25 °C) in the presence of increasing amounts of Cu^{2+} (♦) and Hg^{2+} (●) [logK_{ass} = 6.27(2) and 5.21(1) for $[Cu\mathbf{L^1}]^{2+}$ and $[Hg\mathbf{L^1}]^{2+}$, respectively, evaluated from the spectrofluorimetric data using HypSpec [46].

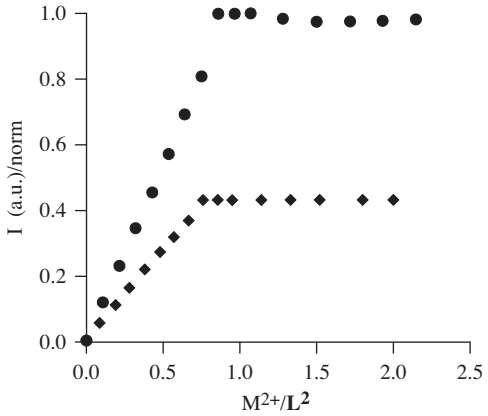

Fig. 4. Normalized fluorescent intensity/molar ratio plots for $\mathbf{L^2}$ (3.08×10^{-5} M, MeCN/H_2O 4:1 v/v, pH 7.0, 25 °C) in the presence of increasing amounts of Zn^{2+} (●) and Cd^{2+} (♦). [logK_{ass} = 7.20(2) and 5.40(2) for $[Zn\mathbf{L^2}]^{2+}$ and $[Cd\mathbf{L^2}]^{2+}$, respectively, evaluated from the spectrofluorimetric data using HypSpec [46].

three other less intense bands at around 260, 300 and 315 nm. In the same solvent mixture $\mathbf{L^2}$ and $\mathbf{L^4}$ exhibit, when excited at 315 nm, an emission band around 380 nm with a very low fluorescent quantum yield, Φ, (0.0083 for $\mathbf{L^2}$ and 0.012 for $\mathbf{L^4}$). This low fluorescence quantum yield can be attributed to a photoinduced electron transfer (PET) process between the tertiary nitrogen atom of the aminopyridine moiety and the quinoline fragments. Significant and comparable changes were observed in the UV–Vis spectra of $\mathbf{L^2}$ and $\mathbf{L^4}$ in MeCN/H_2O (4:1 v/v, 25 °C) solutions buffered with MOPS [MOPS = 3-(*N*-morpholino)propanesulfonic acid] at pH 7.0 upon addition of each metal ion investigated (see Supplementary material, Figs. S5 and S6). In particular, the band at around 230 nm decreases in intensity, shifting to slightly higher wavelengths (see Fig. 3a for the spectrophotometric titration of $\mathbf{L^2}$ with Zn^{2+}). Furthermore, the band at around 260 nm generally decreases and those at 300 and 315 nm very slightly increase in intensity; the presence of well-defined isosbestic point(s) suggests the presence of only two species in equilibrium.

Under the same experimental conditions, with neither of these two ligands does the fluorescence OFF state change upon addition of Cu^{2+}, Hg^{2+} or Pb^{2+}. A significant enhancement of the fluorescence intensity (CHEF effect) was observed upon addition of Zn^{2+} and, to a less extent, upon the addition of Cd^{2+} (see Figs. 3b and 4 for the case of $\mathbf{L^2}$, and Supplementary material for the case of $\mathbf{L^4}$). The effect of Zn^{2+} and Cd^{2+} on the fluorescent intensity emission is less in the case of $\mathbf{L^4}$. In all cases, the inflection point in the fluorescent intensity/molar ratio plots suggests the formation of 1:1 $[M\mathbf{L}]^{2+}$ complexes (M = Zn^{2+}, Cd^{2+}; $\mathbf{L} = \mathbf{L^2}$, $\mathbf{L^4}$).

These results, together with data from the literature [52–60], clearly indicate the quinoline group is an appropriate signalling unit for the construction of selective fluorescent chemosensors for Zn^{2+} over Cd^{2+}; these two metal ions have similar chemical behaviour due to their electronic closed-shell d^{10} configuration and, therefore, they usually cause similar spectral changes after interactions with fluorescent chemosensors. Very recently, the idea has emerged that for Zn^{2+} quinoline-based chemosensors, the CHEF effect for the small Zn^{2+} as compared to the larger Cd^{2+} ion might be determined by the "steric crowding" in the corresponding complexes: an elongation of the Zn–N bond due to "steric crowding" would partially restore the PET quenching mechanism and hence cause a lower CHEF effect for Zn^{2+} relative to Cd^{2+} [55]. Although this hypothesis appears to be confirmed on comparing the optical response of a limited range of quinoline-based chemosensors, extending the comparison to a larger family of molecules reveals that this "steric crowding", if real, is not the only factor to be considered and investigated to fully understand both the

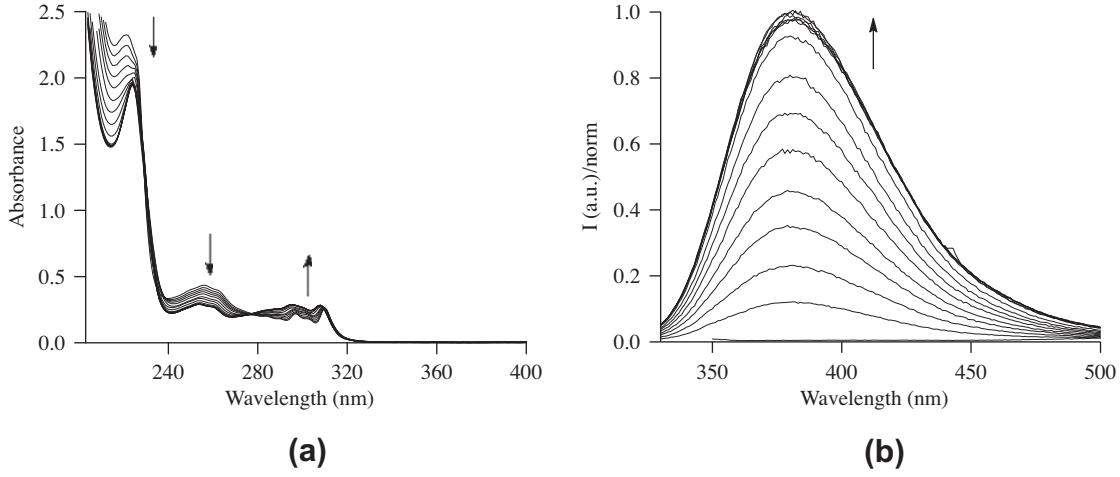

Fig. 3. (a) Changes in the absorption spectrum of $\mathbf{L^2}$ (3.08×10^{-5} M, MeCN/H_2O 4:1 v/v, pH 7.0, 25 °C) upon addition of increasing amounts of Zn^{2+} and (b) changes in the emission spectrum of $\mathbf{L^2}$ (3.08×10^{-5} M, MeCN/H_2O 4:1 v/v, pH 7.0, 25 °C, λ_{ex} = 315, λ_{em} = 380 nm) upon addition of increasing amounts of Zn^{2+}.

ability of quinoline-based fluorescent chemosensors to discriminate Zn^{2+} and Cd^{2+} and the relative intensity of emission in the presence of these two metals.

In Fig. 5, the relative fluorescence intensity [$I_{rel} = I/I_0$] of the ligands **L²** and **L⁴** responding to 1 equiv. of Zn^{2+} (black bar) or Cd^{2+} (grey bar), and the corresponding $I_{rel}(Zn^{2+})/I_{rel}(Cd^{2+})$ ratios (dashed bar), which we can consider as selectivity indexes, are compared to other quinoline-based fluorescent chemosensors from the literature (Scheme 2), many of which are structurally similar to **L²** and **L⁴**. Interestingly (Fig. 5a), most of the quinoline-based chemosensors considered, including **L²** and **L⁴**, are characterized by a zinc(II) complex emission relative to cadmium(II) [$I_{rel}(Zn^{2+})/I_{rel}(Cd^{2+})$] falling within a quite narrow interval from 7.19 (**1 iso-TQEN**) to 1.58 (**TQEN**) [52,54–60]. For Zinquin [60], the value of $I_{rel}(Zn^{2+})/I_{rel}(Cd^{2+})$ is 3.62, not much different from that observed for **L²** (2.35) and **L⁴** (1.75). However, in the case of **L²** though, a much higher relative intensity of emission is observed in the presence of Zn^{2+}.

On going from a "sterically crowded" ligand such as **TQEN** (Table 1) to less sterically crowded ones such as **TQA** or **1 iso-TQEN** for which no significant Zn–$N_{quinoline}$ bond length distortions are observed in the corresponding Zn^{2+} complexes in the solid state (as compared to the mean length for the Zn–$N_{quinoline}$ bonds to quinoline and quinoline-like ligands found in the CSD [52], Table 1) the $I_{rel}(Zn^{2+})/I_{rel}(Cd^{2+})$ ratio increases by a factor of 2.8 or 4.5, respectively. This level of increase, while not negligible, is not outstanding either.

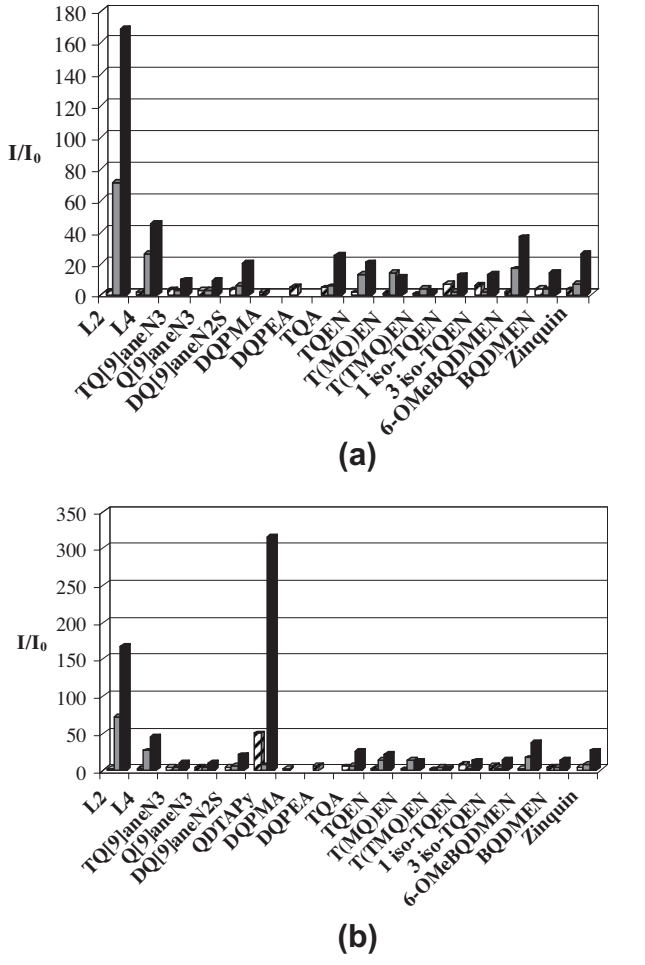

Fig. 5. (a) Relative fluorescence intensity [$I_{rel} = I/I_0$] of **L²** and **L⁴** and the ligands in Scheme 2 except **QDTAPy**, (b) including **QDTAPy**, responding to 1 equiv of Zn^{2+} (black bar) or Cd^{2+} (grey bar), and the corresponding $I_{rel}(Zn^{2+})/I_{rel}(Cd^{2+})$ ratio (dashed bar). I_0 is the emission intensity of the ligands in the absence of metal ions: **TQ[9]aneN3**, **Q[9]aneN3**, **DQ[9]aneN2S** [MeCN/H_2O (1:1 v/v)] [52]; **QDTAPy** [MeCN/H_2O (1:1 v/v)] [53]; **DQPMA**, **DQPEA** (H_2O) [54]; **TQA** [MeOH/H_2O (1:1 v/v)] [55]; **TQEN** [56], **T(MQ)EN**, **T(TMQ)EN** [57], **1 iso-TQEN**, **3 iso-TQEN** [58], **BQDMEN**, **6-OMeBQDMEN** [DMF/H_2O (1:1 v/v)] [59]; **Zinquin** (H_2O) [60].

Also quite intriguing is the higher CHEF effect observed for Cd^{2+} versus Zn^{2+} with **T(MQ)EN**, where the 1:1 complex with Zn^{2+} shows Zn–$N_{quinoline}$ bond length distortions comparable to those observed in the analogous complex with **TQEN** (Table 1, Fig. 5a).

Furthermore, although the Zn–$N_{quinoline}$ bond distances in [Zn(**BQDMEN**)Cl_2] are elongated as compared to those in [Zn(**6-OMeBQDMEN**)H_2O]$^{2+}$ (Table 1), the corresponding $I_{rel}(Zn^{2+})/I_{rel}(Cd^{2+})$ ratios are 4.0 and 2.2, respectively (Fig. 5a).

We have performed DFT calculations and optimized in the gas phase the geometries of the three most likely *pseudo*-octahedral conformers of the 1:1 Zn^{2+} complex with **L²** [C1 (quinolines occupy axial positions, with pyridines and tertiary nitrogen atoms occupying the equatorial plane), C2 (quinoline groups are equatorial), C3 (the two quinoline groups occupy one axial and one equatorial position)] (see Supplementary material, Tables S1–S3, for the orthogonal Cartesian coordinates of C1, C2 and C3). The stability of the three conformers follows the order C1 > C2 > C3, but with energy differences between them of less than 1.5 kcal/mol. The calculated Zn–$N_{quinoline}$ bond distances range between 2.379 and 2.210 Å [C1 (2.379, 2.324 Å), C2 (2.246, 2.245 Å), C3 (2.260, 2.210 Å)], in line with those observed in the solid state for quinoline-based fluorescent chemosensor analogues (Table 1). However, according to the hypothesis of the "steric crowding" described above, only significantly shorter bond distances could explain the high CHEF effect observed for **L²** in the presence of Zn^{2+}. Interestingly, on trying to simulate the presence of a MeCN environment around the complex cation, the optimized metric parameters for very similar conformers of the 1:1 Zn^{2+} complex with **L²** resulting from a conformational search by means of a molecular dynamics procedure, appear to indicate a slight lengthening of the interactions between the quinoline moieties in **L²** and the Zn^{2+} metal ion (bond distances are however comparable with that observed for [Zn(**BQDMEN**)Cl_2] in the solid state (Table 1)), being the conformation with the quinoline groups in *cis* position still more stable than the other two, but only of less than 0.6 kcal/mol (Fig. 6).

In general, we believe that when the signalling unit can coordinate the metal centre a "synergic" cooperation between the signalling and the receptor units must operate to determine the sensitivity and selectivity in the optical response by a fluorescent chemosensor, even though the receptor unit or the chemosensor as a whole is not thermodynamically selective in the host–guest interaction.

What appears to be crucial in determining the emissive behaviour of a fluorescent chemosensor is the manifold of electronic levels associated to the given couple of receptor and signalling units (in this a "synergic" cooperation between the two units should be recognized). This manifold can be selectively perturbed in solution by a metal centre despite a small degree of thermodynamic selectivity in solution, and particular structural features in the solid state. The medium in which the host–guest interaction takes place is also important.

A clear example of this "synergy" between the signalling and receptor units in reaching a selective optical response towards a metal cation comes just from the family of quinoline-based chemosensors for Zn^{2+} under consideration.

For **QDTAPy** (Scheme 2) a $I_{rel}(Zn^{2+})/I_{rel}(Cd^{2+})$ ratio of about 50 is reached with a remarkable sensitivity in the optical response (Fig. 5b) [53], despite the Zn–$N_{quinoline}$ bond distance in the complex [Zn(**QDTAPy**)H_2O]$^{2+}$ (Table 1) being comparable to those in zinc(II) complexes with **TQA**, **1 iso-TQEN** and the other less sterically crowded quinoline-based ligands in Scheme 2. This means that in **QDTAPy** the receptor unit and the signalling unit cooperate

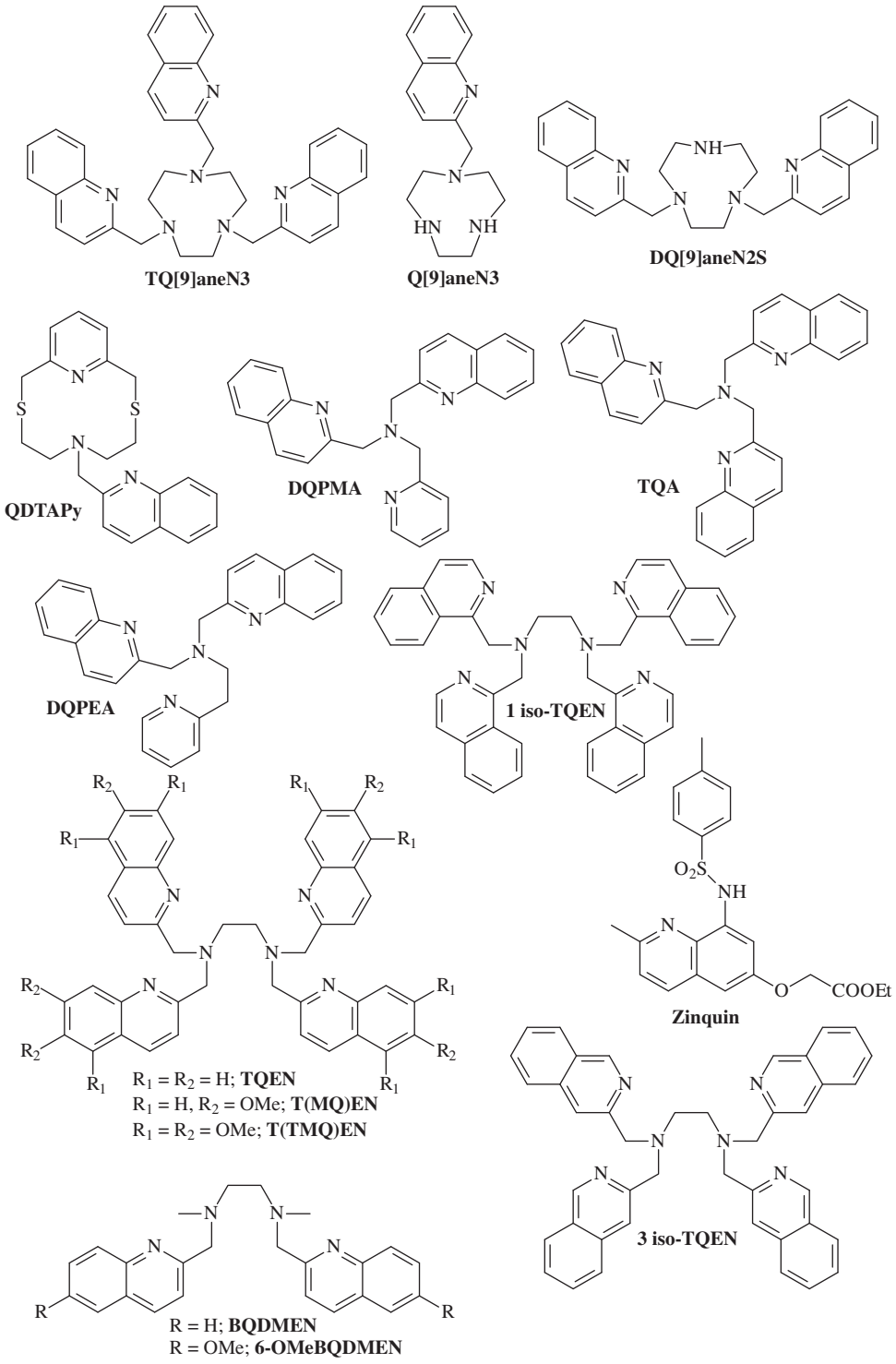

Scheme 2. Quinoline-based fluorescent chemosenors for Zn^{2+} from the literature [52–60].

"synergically" to give a highly selective and sensitive optical response to the presence of zinc(II) despite the fact that this ligand also binds to cadmium(II) (because of its sensing properties, **QDTAPy** has been recently used for the development of a novel flow injection analysis (FIA) system for the determination of traces amounts of Zn^{2+} [61]). Interestingly, although the observed $I_{rel}(Zn^{2+})/I_{rel}(Cd^{2+})$ for $\mathbf{L^2}$ is much lower than that observed for **QDTAPy**, the sensitivity of the optical response to Zn^{2+} [$I_{rel}(Zn^{2+})$] is much higher than that observed for all the other quinoline-based ligands considered, and second only to that recorded for **QDTAPy**, suggesting that $\mathbf{L^2}$ also exhibits "synergic cooperation" between the signalling and the receptor units in sensing Zn^{2+} efficiently.

3.3. Electrochemical response of L^6 and L^7 to the presence of Cu^{2+}, Zn^{2+}, Cd^{2+}, Hg^{2+} or Pb^{2+}

We have also synthesised compounds $\mathbf{L^6}$ and $\mathbf{L^7}$, in order to compare the role played by the receptor units **1** and **2** in both fluorescent and ferrocenyl-based redox chemosensors for metal ions. The electrochemical response of $\mathbf{L^6}$ and $\mathbf{L^7}$ to the presence of

Table 1
Comparison of the M–$N_{quinoline}$ bond lengths (M = Zn^{2+}, Cd^{2+}) in the corresponding structurally characterized complexes of the ligands reported in Scheme 2[a].

Ligands	Zn–$N_{quinoline}$	Mean Zn–$N_{quinoline}$	Cd–$N_{quinoline}$	Mean Cd–$N_{quinoline}$
TQ[9]aneN3	2.2701(15)	2.231	2.371(5)	2.372
	2.2336(14)		2.395(5)	
	2.1897(14)		2.350(6)	
Q[9]aneN3	2.180(4)	2.180		
DQ[9]aneN2S	2.173(5)	2.160	2.320(4)	2.398
	2.149(5)		2.476(3)	
	2.165(5)			
	2.152(5)			
QDTAPy	2.146(2)	2.146(2)		
DQPEA	2.123(5)	2.1475	2.378(4)	2.4595
	2.172(5)		2.541(4)	
TQA		2.132		
TQEN	2.3711(15)	2.2633		
	2.4007(15)			
	2.1543(14)			
	2.1271(14)			
T(MQ)EN	2.157(3)	2.2457		
	2.430(3)			
	2.119(3)			
	2.277(3)			
1 iso-TQEN	2.1269(17)	2.15055		
	2.1742(15)			
3 iso-TQEN	2.1675(16)	2.1589		
	2.1591(17)			
	2.1484(16)			
	2.1608(17)			
BQDMEN	2.4362(15)	2.4362		
6-MeBQDMEN	2.113(3)			
	2.093(3)			

[a] The mean length for M–N bonds to quinoline and quinoline-like ligands found in the CSD is 2.14(6) Å [M = Zn (468 hits)] and 2.36 (5) Å [M = Cd (282 hits)] [52].

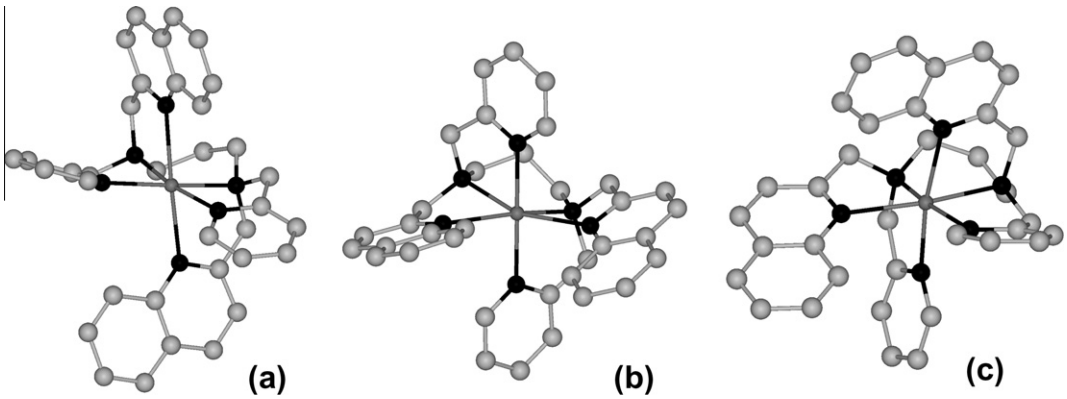

Fig. 6. Most stable conformers of the 1:1 Zn^{2+} complex with $\mathbf{L^2}$ from a conformational search by means of molecular dynamics procedure, optimized at DFT level with implicit simulation of the presence of a MeCN environment (see main text). Zn–$N_{quinoline}$ = 2.452, 2.440 for (a), 2.450, 2.406 for (b) and 2.346, 2.363 Å for (c).

Cu^{2+}, Zn^{2+}, Cd^{2+}, Hg^{2+} or Pb^{2+} as guest metal cation species was investigated by cyclic voltammetry (CV) in MeCN/CH_2Cl_2 (10:1 v/v) mixtures at 25 °C for solubility reasons (ligands do not dissolve in pure MeCN). Cyclic voltammetry of the free ligands reveals only one reversible oxidation wave at $E_{½}$ of 470 and 462 mV versus Ag/AgCl for $\mathbf{L^6}$ and $\mathbf{L^7}$, respectively, corresponding to the Fc/Fc^+ redox couple. These findings indicate that the two ferrocene groups in $\mathbf{L^6}$ and $\mathbf{L^7}$ are electrochemically independent of one another and become oxidized in one step as confirmed by Coulometric studies.

A gradual sequential shift of the oxidation potential was observed for both receptors upon successive addition of $HClO_4$ up to a 1:2 **L**/H^+ molar ratio, with the largest ΔE values of 105 and 98 mV for $\mathbf{L^6}$ and $\mathbf{L^7}$, respectively ($\Delta E = E_{½}^{\text{protonated ionophore}} - E_{½}^{\text{unprotonated ionophore}}$). For both receptors, a one-wave electrochemical behaviour was in general also observed upon addition of 1 equiv. of the metal ions considered, with ΔE values very close to those observed in the presence of $HClO_4$, suggesting that in the presence of metal ions the electrochemical shift is still due to the protonation of the ligands rather than to a metal coordination process. Only in the case of $\mathbf{L^6}$ with Cu^{2+} was two-wave electrochemical behaviour observed, indicating a stronger interaction of this ligand with this metal centre: upon addition of increasing amounts of Cu^{2+}, the redox wave of the free $\mathbf{L^6}$ was gradually replaced by a new reversible wave at more positive potential ($E_{½}$ = 594 mV), the anodically shifted electrochemical wave corresponding to the Fc/Fc^+ redox couple of the $[Cu^{II}\mathbf{L^6}]^{2+}$ species. The current for the new redox couple $[Cu^{II}\mathbf{L^6}]^{2+}/[Cu^{II}\mathbf{L^6}]^{3+}$ increased linearly until one equivalent of the guest metal cation had been added, at which point the reversible oxidation wave corresponding to the uncomplexed ligand disappeared.

The presence of two distinguishable waves in the cyclic voltammograms of $\mathbf{L^6}$ upon addition of Cu^{2+} can be accounted for in terms of an sufficiently higher stability constant for the complex $[Cu^{II}\mathbf{L^6}]^{2+}$ with respect to stability constants of the complexes

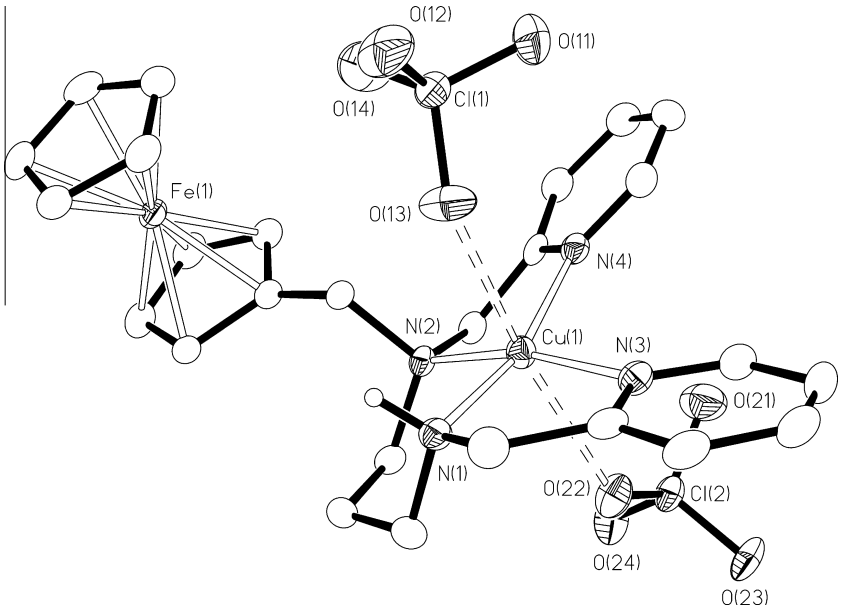

Fig. 7. ORTEP view of the compound [Cu$\mathbf{L}^{8}$$(ClO_4)_2$] with the numbering scheme adopted. Displacement ellipsoids are drawn at 30% probability and hydrogen atoms except that on N(1) have been omitted for clarity. Selected bond lengths and angles: Cu(1)–N(1) 1.996(2), Cu(1)–N(2) 2.033(2), Cu(1)–N(4) 1.986(2), Cu(1)–N(3) 1.988(2), Cu(1)–O(13) 2.740(2), Cu(1)–O(22) 2.599(2) Å; N(1)–Cu(1)–N(2) 92.91(9)°, N(1)–Cu(1)–N(3) 84.29(9)°, N(1)–Cu(1)–N(4) 164.24(9)°, N(1)–Cu(1)–O(13) 76.53(8)°, N(1)–Cu(1)–O(22) 97.63(8)°, N(2)–Cu(1)–N(3) 165.91(9)°, N(2)–Cu(1)–N(4) 83.78(9)°, N(2)–Cu(1)–O(13) 105.76(8)°, N(2)–Cu(1)–O(22) 89.70(7)°, N(3)–Cu(1)–N(4) 102.50(9)°, N(3)–Cu(1)–O(13) 87.07(8)°, N(3)–Cu(1)–O(22) 77.03(8)°, N(4)–Cu(1)–O(13) 89.50(8)°, N(4)–Cu(1)–O(22) 97.76(8)°, O(13)–Cu(1)–O(22) 163.60(7)°.

$[M^{II}\mathbf{L}]^{2+}$ ($\mathbf{L} = \mathbf{L}^{6}$, M = Zn^{2+}, Cd^{2+}, Hg^{2+} or Pb^{2+} ; $\mathbf{L} = \mathbf{L}^{7}$, M = Cu^{2+}, Zn^{2+}, Cd^{2+}, Hg^{2+} or Pb^{2+}) and a sufficiently large difference between the half-wave potentials for the two observed redox couples [62]. According to thermodynamic considerations, the following equation can be derived to describe two-wave behaviour of a redox chemosensor: $E_{½}^{\text{complex}} - E_{½}^{\text{free ionophore}} = (RT/nF)\ln(K_{\text{neutral}}/K_{\text{ox}})$ (K_{neutral} is the metal binding constant for the neutral unoxidized redox-responsive ionophore and K_{ox} is the metal binding constant for its oxidized form). $K_{\text{neutral}}/K_{\text{ox}}$ and $E_{½}^{\text{complex}} - E_{½}^{\text{free ionophore}}$ represent quantitative measures of the perturbation of the redox centre induced by the guest complexation to the receptor unit; both quantities express the ability of the redox chemosensor to selectively respond to the host binding of the guest species [62–64]. In the case of $\mathbf{L}^{6}$ with Cu^{2+} the value obtained for $K_{\text{neutral}}/K_{\text{ox}}$ indicates that in MeCN $\mathbf{L}^{6}$ binds the Cu^{2+} ion *ca.* 10^3 times more strongly than it does its oxidized form $(\mathbf{L}^{6})^{2+}$.

Crystals corresponding to the formulation [Cu$\mathbf{L}^{8}$$(ClO_4)_2$] (see Scheme 1) were unexpectedly obtained from the reaction of $\mathbf{L}^{6}$ with $Cu(ClO_4)_2{\cdot}2H_2O$ in MeCN following partial removal of the solvent from the reaction mixture and slow diffusion of Et_2O vapour into the remaining volume. This complex is formed *via* cleavage of one of the two ferrocenylmethyl pendant arms from the starting ligand $\mathbf{L}^{6}$ to give $\mathbf{L}^{8}$ as complexing agent. In the complex [Cu$\mathbf{L}^{8}$$(ClO_4)_2$] (see Fig. 7) the metal centre occupies a distorted octahedral geometry with the equatorial coordination sites occupied by the four N-donor atoms from $\mathbf{L}^{8}$. The apical positions are occupied by oxygen atoms from two perchlorate counteranions. Due to steric repulsion the two pyridyl rings do not lie on the same plane; as indexes of this distortion, N(3) is displaced 0.98 Å out of the mean plane defined by N(1), N(2) and N(4), and the dihedral angle between the planes defined by the two pyridyl rings is 40.4°. We cannot provide an unambiguous mechanism of this unexpected cleavage of one ferrocenylmethyl pendant arm of $\mathbf{L}^{6}$ upon complexation to Cu^{2+}, but a similar decomposition has been observed for the ligand ferrocenylmethyl-*bis*(2-pyridylethyl)amine in the presence of $ZnBr_2$ [65]: here the authors propose a metal-promoted nucleophilic attack at the benzylic $FcCH_2$ moiety by water, to afford complexed *bis*(2-pyridylethyl)amine and ferrocenylmethanol. However, this mechanism is in doubt because neither in the case of ferrocenylmethyl-*bis*(2-pyridylethyl)amine in the presence of $ZnBr_2$ [65], nor in the case of $\mathbf{L}^{6}$ in the presence of Cu^{2+}, could ferrocenylmethanol be detected in the reaction mixture.

Cyclic voltammetry of the complex [Cu$\mathbf{L}^{8}$$(ClO_4)_2$] in MeCN reveals only a Coulometric-tested one-electron reversible oxidation wave at $E_{½}$ 590 mV versus Ag/AgCl corresponding to the redox wave assigned to the couple $[Cu^{II}\mathbf{L}^{6}]^{2+}/[Cu^{II}\mathbf{L}^{6}]^{3+}$. These findings further support our conclusion that the two ferrocene groups in $\mathbf{L}^{6}$ and $\mathbf{L}^{7}$ are electrochemically independent of one another and are oxidized in a single step.

4. Conclusions

Following previous studies in the field of fluorescent chemosensor design, it is obvious that the developments of efficient fluorescent chemosensors having both binding and sensing selectivity for probing a targeted metal cation in a real matrix, is a challenging task; the kind of selectivity to privilege is the optical response selectivity that can be achieved much easier than the thermodynamic (binding) selectivity [66]. On the other hand, for applications in real matrices that do not contain species which interfere with the binding process of the targeted analyte, the chemosensor does not require strict binding selectivity; alternatively, should this selectivity be required, it could be acquired with the appropriate choice of the medium for the host–guest interaction. On the basis of these general considerations, we advocate that the quest for efficient fluorescent chemosensors for analytical applications follows the "complementary receptor-spacer-fluorophore" supramolecular synthetic approach: given a pre-defined receptor unit (not necessarily the best in the binding process) different signalling units are in turn linked to it in order to establish the best combination showing at least selectivity and sensitivity in the optical response towards a given analyte [66].

The results reported in this paper clearly show that multidentate aminopyridine ligands such as **1** and **2** can be successfully deployed as receptor units in both fluorescent and redox

chemosensors for transition and post-transition metal ions. Although the responses to the presence of the metal ions considered [Cu^{2+}, Zn^{2+}, Cd^{2+}, Hg^{2+}, Pb^{2+}] by the chemosensors presented here appear to be determined more by the intrinsic properties of the signalling units than by the selective binding properties of the receptors, synergism between the receptor and signalling units in determining selectivity and sensitivity in the optical responses appears to be a real possibility.

Acknowledgments

We thank the Università degli Studi di Cagliari for financial support, and the Engineering and Physical Sciences Research Council (UK) for the provision of the X-ray diffractometer.

Appendix A. Supplementary material

CCDC 829573 contains the supplementary crystallographic data for this paper. These data can be obtained free of charge from The Cambridge Crystallographic Data Centre via www.ccdc.cam.ac.uk/data_request/cif. Further material deposited: changes in the absorption spectrum of $\mathbf{L^1}$–$\mathbf{L^5}$ (MeCN/H_2O 4:1 v/v, 25 °C) upon addition of increasing amounts of Cu^{2+} and Hg^{2+} (Figs. S1–S3); normalized fluorescent intensity/molar ratio plots for $\mathbf{L^3}$ and $\mathbf{L^5}$ (MeCN/H_2O 4:1 v/v, 25 °C) in the presence of increasing amounts of Cu^{2+} and Hg^{2+} (Fig. S4); changes in the absorption spectrum of $\mathbf{L^2}$ and $\mathbf{L^4}$ (MeCN/H_2O 4:1 v/v, 25 °C) upon addition of increasing amounts of Zn^{2+} and Cd^{2+} (Figs. S5 and S6); normalized fluorescent intensity/molar ratio plots for $\mathbf{L^4}$ (MeCN/H_2O 4:1 v/v, 25 °C) in the presence of increasing amounts of Cd^{2+} and Zn^{2+} (Fig. S7); optimized geometries calculated for $[Zn\mathbf{L^2}]^{2+}$ at DFT level in orthogonal Cartesian coordinate format (Tables S1–S3). Supplementary data associated with this article can be found, in the online version, at doi:10.1016/j.ica.2011.09.025.

References

[1] A.W. Czarnik, Acc. Chem. Res. 27 (1994) 302.
[2] A.W. Czarnik, J.-P. Desvergene (Eds.), Chemosensors of Ions and Molecular Recognition, NATO ASI Seies C, vol. 492, Kluwer Academic Publishers, Dordrecht, NL, 1997.
[3] A.P. de Silva, H.Q.G. Gunaratne, T. Gunnlaugsson, A.J.M. Huxley, C.P. McCoy, J.T. Rademacher, T.E. Rice, Chem. Rev. 97 (1997) 1515.
[4] E. Kimura, T. Koike, Chem. Soc. Rev. 27 (1998) 179.
[5] R. Bergonzi, L. Fabbrizzi, M. Licchelli, C. Mangano, Coord. Chem. Rev. 170 (1998) 31.
[6] Coord. Chem. Rev. 205 (2000) (Special Issue on Luminescent Sensors).
[7] K. Rurack, Spectrochim. Acta, Part A 57 (2001) 2161.
[8] S.L. Wiskur, A. Haddou, J.J. Lavigne, E.V. Anslyn, Acc. Chem. Res. 34 (2001) 963.
[9] K. Parack, U. Resch-Genger, Chem. Soc. Rev. 31 (2002) 116.
[10] C.W. Rogers, M.O. Wolf, Coord. Chem. Rev. 233–234 (2002) 341.
[11] L. Fabbrizzi, M. Licchelli, A. Taglietti, Dalton Trans. (2003) 3471.
[12] R. Martinez-Máñez, F. Sancenon, Chem. Rev. 103 (2003) 4419.
[13] L. Prodi, New J. Chem. 29 (2005) 20.
[14] J. Mater. Chem. 15 (2005) (Special Issue on Fluorescent Sensors).
[15] A. Amendola, L. Fabbrizzi, F. Foti, M. Licchelli, C. Mangano, P. Pallavicini, A. Poggi, D. Sacchi, A. Taglietti, Coord. Chem. Rev. 250 (2006) 273.
[16] J.S. Kim, D.T. Quang, Chem. Rev. 207 (2007) 3780.
[17] L. Basabe-Desmonts, D.N. Reinhoudt, M. Crego-Calama, Chem. Soc. Rev. 36 (2007) 993.
[18] C. Lodeiro, F. Pina, Coord. Chem. Rev. 253 (2009) 1353.
[19] P.S. Pallavicini, Y.A. Diaz-Fernandez, L. Pasotti, Coord. Chem. Rev. 253 (2009) 2226.
[20] C. Lodeiro, J.L. Capelo, J.C. Mejuto, E. Oliveira, H.M. Santos, B. Pedras, C. Nuñez, Chem. Soc. Rev. 39 (2010) 2948.
[21] M.E. Moragues, R. Martínez-Máñez, F. Sancenón, Chem. Soc. Rev. 40 (2011) 2593.
[22] G. Anderegg, N.G. Podder, P. Bläuenstein, M. Hangartner, H. Stünzi, J. Coord. Chem. 4 (1974) 267.
[23] E.D. McKenzie, F.S. Stephens, Inorg. Chim. Acta 42 (1980) 1.
[24] H.R. Fischer, D.J. Hodgson, K. Michelsen, E. Pedersen, Inorg. Chim. Acta 88 (1984) 143.
[25] J.A.R. Hartman, A.L. Kammier, R.J. Spracklin, W.H. Pearson, M.Y. Combariza, R.W. Vachet, Inorg. Chim. Acta 357 (2004) 1141.
[26] J. Glerup, P.A. Goodson, D.J. Hodgson, K. Michelsen, Inorg. Chem. 34 (1995) 6255.
[27] K. Kanamori, A. Kyotoh, K. Fujimoto, K. Nagata, H. Suzuki, K.-I. Okamoto, Bull. Chem. Soc. Jpn 74 (2001) 2113.
[28] E.M. Nolan, S.J. Lippard, Acc. Chem. Res. 42 (2009) 193.
[29] A. Credi, L. Prodi, Spectrochim. Acta 54 (1998) 159.
[30] M.A. Heinrichs, D.J. Hodgson, K. Michelsen, E. Pedersen, Inorg. Chem. 23 (1984) 3174.
[31] O. Yamauchi, H. Seki, T. Shoda, Bull. Chem. Soc. Jpn 56 (1983) 3258.
[32] A.J. Blake, J.P. Danks, A. Harrison, S. Parsons, P. Schooler, G. Whittaker, M. Schröder, J. Chem. Soc., Dalton Trans. (1998) 2335.
[33] D. Lednicer, C.R. Hauser, Org. Synth. 40 (1960) 31.
[34] S. Aoki, H. Kawatani, T. Goto, E. Kimura, M. Shiro, J. Am. Chem. Soc. 123 (2001) 1123.
[35] G. M. Sheldrick, SHELXL97, Acta Crystallogr., Sect. A 64 (2008) 112.
[36] A. Altomare, G. Cascarano, C. Giacovazzo, A. Guagliardi, M.C. Burla, G. Polidori, M. Camalli, J. Appl. Crystallogr. 27 (1994) 435.
[37] C.J. Cramer, Essentials of Computational Chemistry, second ed., Wiley, Chechester (England), 2004 (chapter 8).
[38] GAUSSIAN 09, Revision A.02, M.J. Frisch, G.W. Trucks, H.B. Schlegel, G.E. Scuseria, M.A. Robb, J.R. Cheeseman, G. Scalmani, V. Barone, B. Mennucci, G.A. Petersson, H. Nakatsuji, M. Caricato, X. Li, H.P. Hratchian, A.F. Izmaylov, J. Bloino, G. Zheng, J.L. Sonnenberg, M. Hada, M. Ehara, K. Toyota, R. Fukuda, J. Hasegawa, M. Ishida, T. Nakajima, Y. Honda, O. Kitao, H. Nakai, T. Vreven, J.A. Montgomery Jr., J.E. Peralta, F. Ogliaro, M. Bearpark, J.J. Heyd, E. Brothers, K.N. Kudin, V.N. Staroverov, R. Kobayashi, J. Normand, K. Raghavachari, A. Rendell, J.C. Burant, S.S. Iyengar, J. Tomasi, M. Cossi, N. Rega, J.M. Millam, M. Klene, J.E. Knox, J.B. Cross, V. Bakken, C. Adamo, J. Jaramillo, R. Gomperts, R.E. Stratmann, O. Yazyev, A.J. Austin, R. Cammi, C. Pomelli, J.W. Ochterski, R.L. Martin, K. Morokuma, V.G. Zakrzewski, G.A. Voth, P. Salvador, J.J. Dannenberg, S. Dapprich, A.D. Daniels, Ö. Farkas, J.B. Foresman, J.V. Ortiz, J. Cioslowski, D.J. Fox, Gaussian, Inc., Wallingford CT, 2009.
[39] C. Adamo, V. Barone, J. Chem. Phys. 108 (1998) 664.
[40] A. Schäfer, H. Horn, R. Ahlrichs, J. Chem. Phys. 97 (1992) 2571.
[41] L.E. Roy, P.J. Hay, R.L. Martin, J. Chem. Theory Comput. 4 (2008) 1029.
[42] W.L. Jorgensen, D.S. Maxwell, J. Tirado-Rives, J. Am. Chem. Soc. 118 (1996) 11225.
[43] (a) A.D. Becke, J. Chem. Phys. 98 (1993) 1372;
(b) A.D. Becke, J. Chem.Phys. 98 (1993) 5648;
(c) B. Miehlich, A. Savin, H. Stoll, H. Preuss, Chem. Phys. Lett. 157 (1989) 200.
[44] **jaguar** version 7.8, Schrödinger L.L.C., New York, 2011. http://www.schrodinger.com.
[45] M.C. Cortis, R.A. Friesner, J. Comput. Chem. 18 (1997) 1591.
[46] P. Gans, A. Sabatini, A. Vacca, Talanta 43 (1996) 1739. log K_{35S} = 5.68(1), 4.91(1), 5.37(1), 5.22 (1), 5.97 (2) and 4.86(1) for $[Cu\mathbf{L^3}]^{2+}$, $[Hg\mathbf{L^3}]^{2+}$, $[Cu\mathbf{L^5}]^{2+}$, $[Hg\mathbf{L^5}]^{2+}$, $[Zn\mathbf{L^4}]^{2+}$ and $[Cd\mathbf{L^4}]^{2+}$, respectively.
[47] L. Prodi, F. Bolletta, M. Montalti, N. Zaccheroni, Eur. J. Inorg. Chem. (1999) 901.
[48] M.C. Aragoni, M. Arca, A. Bencini, A.J. Blake, C. Caltagirone, A. Decortes, F. Demartin, F.A. Devillanova, E. Faggi, L.S. Dolci, A. Garau, F. Isaia, V. Lippolis, L. Prodi, C. Wilson, B. Valtancoli, N. Zaccheroni, Dalton Trans. (2005) 2994.
[49] A.J. Blake, A. Bencini, C. Caltagirone, G. De Filippo, L.S. Dolci, A. Garau, F. Isaia, V. Lippolis, P. Mariani, L. Prodi, M. Montalti, N. Zaccheroni, C. Wilson, Dalton Trans. (2004) 2771.
[50] G. Xue, J.S. Bradshaw, H. Song, R.T. Bronson, P.B. Savage, K.E. Krakowiak, R.M. Izatt, L. Prodi, M. Montalti, N. Zaccheroni, Tetrahedron 57 (2001) 87.
[51] T. Koike, T. Abe, M. Takahashi, K. Ohtani, E. Kimura, M. Shiro, Dalton Trans. (2002) 1764.
[52] M. Mameli, M.C. Aragoni, M. Arca, M. Atzori, A. Bencini, C. Bazzicalupi, A.J. Blake, C. Caltagirone, F.A. Devillanova, A. Garau, M.B. Hursthouse, F. Isaia, V. Lippolis, B. Valtancoli, Inorg. Chem. 48 (2009) 9236.
[53] M.C. Aragoni, M. Arca, A. Bencini, A.J. Blake, C. Caltagirone, A. Danesi, F.A. Devillanova, A. Garau, T. Gelbrich, M.B. Hursthouse, F. Isaia, V. Lippolis, M. Mameli, P. Mariani, B. Valtancoli, C. Wilson, Inorg. Chem. 46 (2007) 4548.
[54] W. Gan, S.B. Jones, J.H. Reibenspies, R.D. Hancock, Inorg. Chim. Acta 358 (2005) 3958.
[55] N.J. Williams, W. Gan, J.H. Reibenspies, R.D. Hancock, Inorg. Chem. 48 (2009) 1407.
[56] Y. Mikata, M. Wakamatsu, S. Yano, Dalton Trans. (2005) 545.
[57] Y. Mikata, M. Wakamatsu, A. Kawamura, N. Yamanata, S. Yano, A. Odani, K. Morihiro, S. Tamotsu, Inorg. Chem. 45 (2006) 9262.
[58] Y. Mikata, A. Yamanata, S. Yano, Inorg. Chem. 47 (2008) 7295.
[59] Y. Mikata, Y. Yamashita, A. Kawamura, H. Konno, Y. Miyamoto, S. Tamatsu, Dalton Trans. (2009) 3800.
[60] M.C. Kimber, I.B. Mahadevan, S.F. Lincoln, A.D. Ward, E.R.T. Tiekink, J. Org. Chem. 65 (2000) 8204.
[61] M. Shamsipur, M.M. Zahedi, G. De Filippo, V. Lippolis, Talanta 85 (2011) 687.
[62] J.C. Medina, T.T. Goodnow, M.T. Rojas, J.L. Atwood, B.C. Lynn, A.E. Kaifer, G.W. Gokel, J. Am. Chem. Soc. 114 (1992) 10583.
[63] P.D. Beer, P.A. Gale, G.Z. Chen, Coord. Chem. Rev. 185–186 (1999) 3.
[64] P.D. Beer, P.A. Gale, G.Z. Chen, J. Chem. Soc., Dalton Trans. (1999) 1897.
[65] Q. Folshade Mokuolu, C.A. Kilner, S.A. Barrett, P.C. McGowan, M.A. Halcrow, Inorg. Chem. 44 (2005) 4136.
[66] A. Bencini, V. Lippolis, Coord. Chem. Rev. (2011). doi:10.1016/j.ccr.2011.05.015.